

Article

Synthetic ShK-like Peptide from the Jellyfish *Nemopilema nomurai* Has Human Voltage-Gated Potassium-Channel-Blocking Activity

Ye-Ji Kim ^{1,2}, Yejin Jo ³, Seung Eun Lee ⁴, Jungeun Kim ⁵, Jae-Pil Choi ⁵, Nayoung Lee ³, Hyokyong Won ³, Dong Ho Woo ^{1,2,*} and Seungshic Yum ^{3,6,*}

- ¹ Department of Advanced Toxicology Research, Korea Institute of Toxicology (KIT), Daejeon 34114, Republic of Korea; yeji.kim@kitox.re.kr
- ² Human and Environmental Toxicology, University of Science and Technology, Daejeon 34114, Republic of Korea
- ³ Ecological Risk Research Division, Korea Institute of Ocean Science and Technology (KIOST), Geoje 53201, Republic of Korea; ye9302@kiost.ac.kr (Y.J.); dylee@kiost.ac.kr (N.L.); bluepigret@naver.com (H.W.)
- ⁴ Research Animal Resource Center, Korea Institute of Science and Technology (KIST), Seoul 02792, Republic of Korea; selee@kist.re.kr
- ⁵ Personal Genomics Institute (PGI), Genome Research Foundation (GRF), Cheongju 28160, Republic of Korea; jungeunkim079@gmail.com (J.K.); casperch@gmail.com (J.-P.C.)
- ⁶ KIOST School, University of Science and Technology, Geoje 53201, Republic of Korea
- * Correspondence: dongho.woo@kitox.re.kr (D.H.W.); syum@kiost.ac.kr (S.Y.)

Abstract: We identified a new human voltage-gated potassium channel blocker, NnK-1, in the jellyfish *Nemopilema nomurai* based on its genomic information. The gene sequence encoding NnK-1 contains 5408 base pairs, with five introns and six exons. The coding sequence of the NnK-1 precursor is 894 nucleotides long and encodes 297 amino acids containing five presumptive ShK-like peptides. An electrophysiological assay demonstrated that the fifth peptide, NnK-1, which was chemically synthesized, is an effective blocker of hKv1.3, hKv1.4, and hKv1.5. Multiple-sequence alignment with cnidarian Shk-like peptides, which have Kv1.3-blocking activity, revealed that three residues (³Asp, ²⁵Lys, and ³⁴Thr) of NnK-1, together with six cysteine residues, were conserved. Therefore, we hypothesized that these three residues are crucial for the binding of the toxin to voltage-gated potassium channels. This notion was confirmed by an electrophysiological assay with a synthetic peptide (NnK-1 mu) where these three peptides were substituted with ³Glu, ²⁵Arg, and ³⁴Met. In conclusion, we successfully identified and characterized a new voltage-gated potassium channel blocker in jellyfish that interacts with three different voltage-gated potassium channels. A peptide that interacts with multiple voltage-gated potassium channels has many therapeutic applications in various physiological and pathophysiological contexts.

Keywords: toxin; venom; jellyfish; Cnidaria; genomic information; electrophysiology



Citation: Kim, Y.-J.; Jo, Y.; Lee, S.E.; Kim, J.; Choi, J.-P.; Lee, N.; Won, H.; Woo, D.H.; Yum, S. Synthetic ShK-like Peptide from the Jellyfish *Nemopilema nomurai* Has Human Voltage-Gated Potassium-Channel-Blocking Activity. *Mar. Drugs* **2024**, *22*, 217. <https://doi.org/10.3390/md22050217>

Academic Editors: Elva Morretta, Maria Chiara Monti and Raffaella Belvedere

Received: 27 April 2024

Revised: 8 May 2024

Accepted: 10 May 2024

Published: 13 May 2024



Copyright: © 2024 by the authors. Licensee MDPI, Basel, Switzerland. This article is an open access article distributed under the terms and conditions of the Creative Commons Attribution (CC BY) license (<https://creativecommons.org/licenses/by/4.0/>).

1. Introduction

Technological advances in genome and transcriptome sequencing, bioinformatics, and the chemical synthesis of peptides and proteins provide unprecedented opportunities to isolate potential pharmacomedical compounds from venoms. Cnidaria is a representative group of venomous marine animals. Various kinds of potentially toxic proteins and peptides have been reported in cnidarians after transcriptomic and/or proteomic analyses, and they have been reviewed recently [1–4]. The functional assays of some toxic components deduced from transcriptomic analyses have been undertaken with chemically synthesized materials rather than purified toxic components [5]. *Nemopilema nomurai* venom has great potential utility in this regard because its genomic information is available [6], and its

venom extracts have shown various therapeutic properties, including antimetastatic [7] and anticancer effects [8]. Therefore, it is highly likely that jellyfish venom contains many types of ion channel blockers.

Voltage-gated potassium channels play critical roles in regulating the electrical activity of cells, particularly in neurons and muscle cells [9]. Investigating the binding specificity and selectivity of toxins to different potassium channel subtypes may provide insights into the structural determinants of channel–peptide interactions and aid in the design of more selective modulators or drugs targeting specific potassium channel isoforms. A comprehensive review of Kv1 channels targeting toxins from marine animals is available [10]. Among Kv1 channels, the activation of the voltage-gated potassium channel Kv1.3 in human T and B lymphocytes is related to the development of autoimmune diseases [11–13]. Therefore, Kv1.3 has become a therapeutic target for the treatment of these diseases [14–16].

Among the effective potassium channel blockers, an ShK-186 analog was the first candidate drug to display clinically useful traits [17,18]. The ShK peptide was identified in the sea anemone *Stichodactyla helianthus* [19]. In brief, it consists of 35 amino acid residues, including six cysteines bridged by three disulfide bonds [20], and it blocks voltage-dependent potassium channels. Since its discovery, other toxic ShK-like peptides have been detected and characterized in other sea anemone species [21–25] and corals [5,26]. ShK-like peptides have also been reported in jellyfish species [27,28]; however, their biological function has not yet been revealed.

Recently, we identified seven ShK-like peptide precursor genes in the genomic information of the jellyfish *N. nomurai* [6]. In the present study, we describe the structure of an open reading frame (ORF) among these seven precursor genes and its deduced amino acid sequence, which contains five putative ShK-like peptides. The fifth peptide, NnK-1, was chemically synthesized, and we investigated whether it has voltage-gated-potassium-channel-blocking activity in the isoforms and subtypes of human potassium channels. For this purpose, we used an internal ribosome entry site (IRES)-containing vector to separately express the human potassium channel genes (*hKv1.1*, *hKv1.3*, *hKv1.4*, *hKv1.5*, *hKv3.1*, and *hKv11.1*) and the enhanced green fluorescent protein (EGFP) gene to avoid generating an EGFP–Kv fusion protein. The current amplitudes at the voltage increments of +50 mV were significantly reduced in cells expressing synthetic NnK-1. Our findings contribute to the characterization of toxins with potential voltage-gated-ion-channel-blocking functions, which could be developed for therapeutic applications.

2. Results and Discussion

2.1. Genomic DNA and Transcript Sequences of NnK-1 Precursor Gene

The whole gene sequence of the NnK-1 precursor contains 5408 base pairs with six distinct exons, and the classical 5' donor (GT) and 3' acceptor (AG) splice sites are present at each exon–intron boundary (Figure 1).

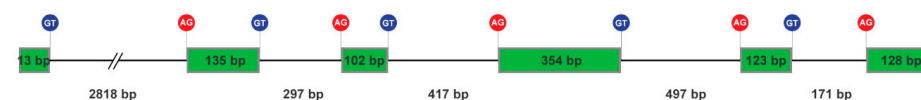


Figure 1. Organization of the *Nemopilema nomurai* NnK-1 precursor gene, which contains six distinct exons (green).

A transcript encoding an ShK-like peptide was predicted. Figure 2 shows the sequence structure of 894 base pairs encoding the 297 amino acid residues of an ORF. Five presumptive ShK-like peptides (printed in bold) were detected in the protein. All five peptides had mono- or dibasic amino acid residues upstream of their N-termini and downstream of their C-termini, and these were responsible for peptide precursor conversion [29]. Multiple ShK-like peptides are also tandemly arranged in a single coding sequence in the genomes of jellyfish and sea anemones [30]. Therefore, a more efficient process for producing cysteine-

rich peptide toxins may have evolved at some point during the evolutionary history of cnidarians, possibly through gene duplication.

```

ATG ATT GCT AGC ATT CTG CTA ACA TAT ATC CAT GCA AGT ATG GAC 45
M I A S I L L T Y I H A S M D 15
AAT AGA GAA TTC CCA TTA AAG CCC GCC TGC GTA GAA GCA CAG GAA 90
N R E F P L K P A C V E A Q E 30
CAC CCC TTC GCG AAC TGC AGA AAG CTC CGA CTT GCT GGG GAG TGC 135
H P F A N C R K L R L A G E C 45
AAA TCA AAT CGC GTG AAG AAA TGG TGT CCA AAG ACG TGC AAG TAT 180
K S N R V K K W C P K T C K Y 60
TGC ATA GAA ACG AGA GCT GCA GCC CCA GTT CAA TGC CAT TTG ACG 225
C I E T R A A A P V Q C H L T 75
ACA TTT GGA TGC TGT GCT GAT GGC ATA AAA GCG GCC AAA GGG AAG 270
T F G C C A D G I K A A K G K 90
AAT GGA CTT GGC TGC CCA GAA AAT TGC AAA GAC TAC GAT AAA AGA 315
N G L G C P E N C K D Y D K R 105
AAC TGC AAG CAC TAT GCC TCC CAA AAA TTC TGT GAA GAT AAA TCC 360
N C K H Y A S Q K F C E D K S 120
TAC TTC GCA ATC ATG AGA AGG CTG TGC CCA GAG TCG TGC TTC ATG 405
Y F A I M R R L C P E S C F M 135
TGC GGA AAG AAA ATT GTC GAT AAT TGT TAC AAC TTG GTT TCG GAT 450
C G K K I V D N C Y N L V S D 150
TCG TAC TGC AAG AAG CTT GAA CGT ATG GGT TTC TGC AGA AGC AAG 495
S Y C K K L E R M G F C R S K 165
ACA ATG CAG GGT AAA ATG AGG AAA TAC TGT GCT CTC ACC TGC GAG 540
T M Q G K M R K Y C A L T C E 180
GCA TGT GGC AAC AAC GTG CCG AAA CTG ACG GAA GTG ATG CCG AAG 585
A C G N N V P K L T E V M P K 195
TGT GCC GGA GTC GGT TGC TGT TGG GAT GAC GTC ACC CCG ATC AAT 630
C A G V G C C W D D V T P I N 210
AAA GGC TGT CCA GTA TGC AAA AAC AAA GGT GAA GGC ACT TTT TGC 675
K G C P V C K N K G E G T F C 225
CAA CGA TTC AAG AGT GAT TGC TTC CAC ATC GAC AGG CTT CCA TCT 720
Q R F K S D C F H I D R L P S 240
GTA CAA ATG AAA ACT ATA TGC TCA GAG ACA TGT GGA ATA TGT GAC 765
V Q M K T I C S E T C G I C 255
TTA CGA ACA TGC AAG GAT CAT CAT ACC TAC GGT GTT TAT TGC AAA 810
L R T C K D H H T Y G V Y C K 270
GAC TGG AAG TCA TCT GGA GAA TGC AAG AAG AAC CCC AAA GGA ATG 855
D W K S S G E C K K N P K G M 285
AGA CAT TTC TGC AGG AAG ACC TGT GGG TTC TGT CGG TAA 894
R H F C R K T C G F C R * 297

```

Figure 2. Transcript sequence of the NnK-1-encoding gene and the deduced amino acid sequences. The amino acid sequences of the five ShK-like peptides are printed in bold. NnK-1 is printed in red.

2.2. Voltage-Gated Potassium Channel Blockade Function of NnK-1

We constructed six kinds of pAAV-CMV-hKv-IRES2-EGFP, which included each of the *hKv1.1*, *hKv1.3*, *hKv1.4*, *hKv1.5*, *hKv3.1*, and *hKv11.1* genes, to allow the activity of these potassium channels to be measured separately without interference by green fluorescent protein (GFP). We mainly focused on measuring the activity of hKv1.3. After the transfection of pAAV-CMV-hKv1.3-IRES2-EGFP, the fluorescence of GFP was highly visible (Figure 3A), and the currents from the HEK293 cells expressing AAV-CMV-hKv1.3-IRES2-EGFP were clearly recorded when the specified voltage steps were applied, unlike in the untransfected HEK293 cells (Figure 3B,C). The current-voltage (IV) recorded in the HEK cells expressing hKv1.3 showed a significant difference in the interaction between the expressed hKv1.3 and the voltage steps (Figure 3C). The hKv1.3 current amplitudes at 50 mV were significantly higher than those of the untransfected HEK293 cells (Figure 3D). The current of hKv1.3 was significantly reduced by treatment with 0.01, 1, 100, or 500 nM

synthetic ShK peptide, which was first identified in the sea anemone *S. helianthus* [19] (Figure 3E–G, * $p < 0.05$, ** $p < 0.01$, *** $p < 0.001$, **** $p < 0.0001$), as well as by treatment with 0.01, 1, 100, or 500 nM Psora4, a pan-Kv1.3 blocker (Figure 3H–J, * $p < 0.05$, ** $p < 0.01$, *** $p < 0.001$, **** $p < 0.0001$). Importantly, the current amplitude of hKv1.3 was also significantly reduced through the application of 0.01, 1, 100, or 500 nM NnK-1 (Figure 3K–M, * $p < 0.05$, ** $p < 0.01$, **** $p < 0.0001$), suggesting that NnK-1 is a candidate inhibitor of hKv1.3. To assess whether the toxicity of ShK and NnK-1 affected their inhibitory effect on hKv1.3, we measured the cell viability in the untransfected HEK293 cells and hKv1.3-transfected HEK293 cells. There was no difference in 1 h treatments with 0.01, 1, 100, and 500 nM ShK and NnK-1 in the untransfected HEK293 cells and hKv1.3-transfected HEK293 cells (Figure 3N–Q).

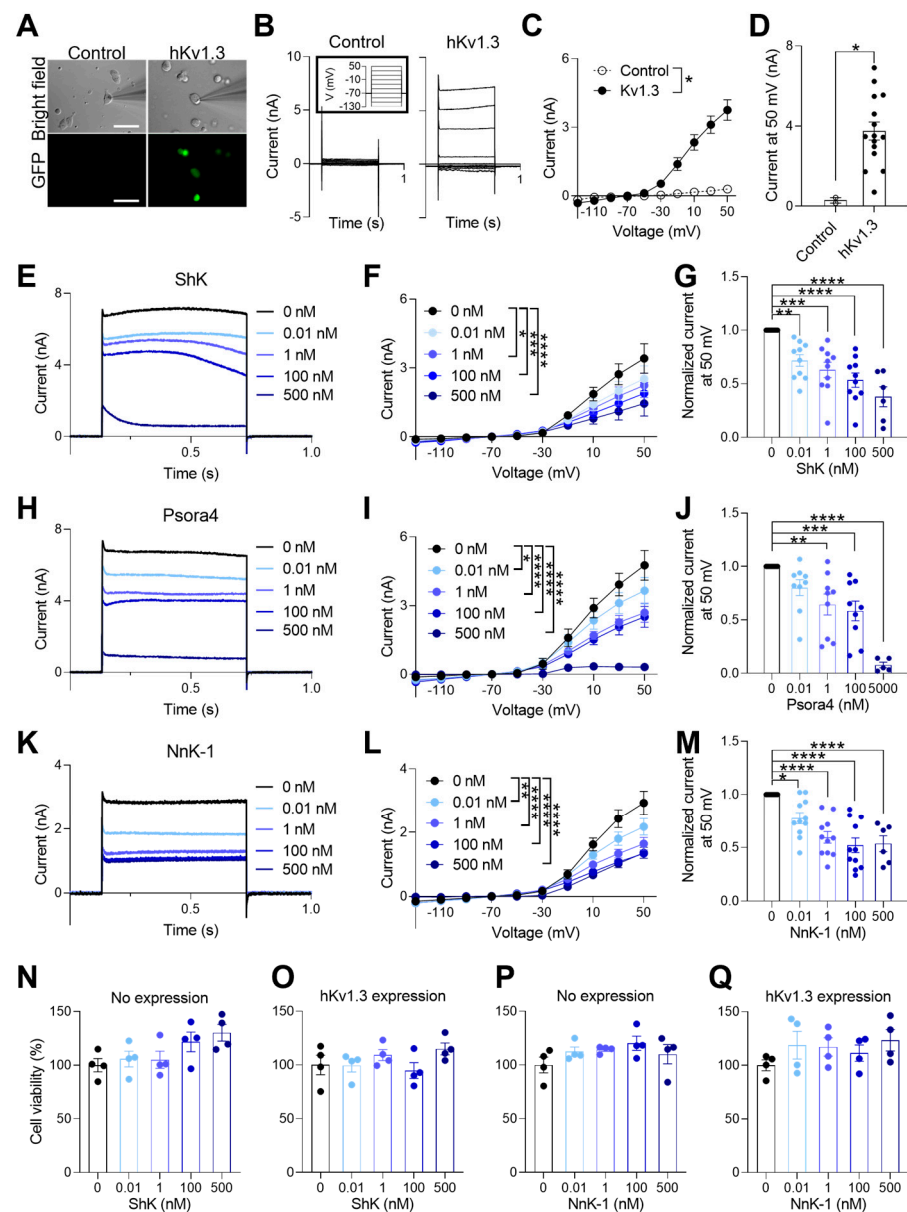


Figure 3. Inhibitory effect of NnK-1 on the activation of hKv1.3 channels. (A) Bright-field images of glass pipettes used for the patch clamp of the HEK293 cells (upper panels) and fluorescence microscopic images of the cells (lower panel) without (left panel) and with GFP (right panel) showing the expression of AAV-CMV-hKv1.3-IRES2-EGFP. Scale bar, 50 μm . (B) Current amplitudes ranging

from -130 to 50 mV in the increments of 20 mV (10 steps) without (left) and with hKv1.3 (right). The inset indicates 10 voltage steps. (C) Representative current–voltage (IV) curves without (\circ) and with hKv1.3 (\bullet). Unpaired *t*-test, $* p < 0.05$. (D) The summary bar graphs of current amplitudes without and with hKv1.3 expression at 50 mV. Unpaired *t*-test, $* p < 0.05$. (E) hKv1.3-mediated currents at 50 mV in the presence of the indicated concentrations of ShK (0, 0.01, 1, 100, or 500 nM). (F) Representative IV curves in the presence of ShK (0, 0.01, 1, 100, or 500 nM). Two-way ANOVA, interaction between the voltage and group $F(36, 410) = 1.269$, $p = 0.14$; voltage $F(9, 410) = 65.13$, $p < 0.0001$; group $F(4, 410) = 6.148$, $p < 0.0001$, followed by Dunnett’s post hoc test, $* p < 0.05$, 0 vs. 1 nM, $*** p < 0.001$, 0 vs. 100 nM, $**** p < 0.0001$, 0 vs. 500 nM. (G) The summary bar graphs of current amplitudes at 50 mV in the presence of ShK (0, 0.01, 1, 100, or 500 nM). One-way ANOVA, $F(4, 41) = 13.51$, $p < 0.0001$, followed by Dunnett’s post hoc test, $** p < 0.01$, 0 vs. 0.01 nM, $*** p < 0.001$, 0 vs. 1 nM, $**** p < 0.0001$, 0 vs. 100 nM, 0 vs. 500 nM. (H) hKv1.3-mediated currents at 50 mV in the presence of the indicated concentrations of Psora4 (0, 0.01, 1, 100, or 500 nM). (I) Representative IV curves in the presence of Psora4 (0, 0.01, 1, 100, or 500 nM). Two-way ANOVA, interaction between the voltage and group $F(36, 360) = 4.805$, $p < 0.0001$; voltage $F(9, 360) = 88.19$, $p < 0.0001$; group $F(4, 360) = 25.38$, $p < 0.0001$, followed by Dunnett’s post hoc test, $* p < 0.05$, 0 vs. 0.01 nM, $**** p < 0.0001$, 0 vs. 1 nM, 0 vs. 100 nM, 0 vs. 500 nM. (J) The summary bar graphs of current amplitudes at 50 mV in the presence of Psora4 (0, 0.01, 1, 100, or 500 nM). One-way ANOVA, $F(4, 36) = 15.58$, $p < 0.0001$, followed by Dunnett’s post hoc test, $** p < 0.01$, 0 vs. 1 nM, $*** p < 0.001$, 0 vs. 100 nM, $**** p < 0.0001$, 0 vs. 500 nM. (K) Representative traces in the presence of the indicated concentrations of NnK-1 (0, 0.01, 1, 100, or 500 nM). (L) Representative IV curves in the presence of NnK-1 (0, 0.01, 1, 100, or 500 nM). Two-way ANOVA, the interaction between the voltage and group $F(36, 450) = 5.257$, $p < 0.0001$; voltage $F(9, 450) = 183.1$, $p < 0.0001$; group $F(4, 450) = 21.75$, $p < 0.0001$, followed by Dunnett’s post hoc test, $** p < 0.01$, 0 vs. 0.01 nM, $**** p < 0.0001$, 0 vs. 1 nM, 0 vs. 100 nM, 0 vs. 500 nM. (M) The summary bar graphs of current amplitudes at 50 mV in the presence of NnK-1 (0, 0.01, 1, 100, or 500 nM). One-way ANOVA, $F(4, 45) = 14.39$, $p < 0.0001$, followed by Dunnett’s post hoc test, $* p < 0.05$, 0 vs. 0.01 nM, $**** p < 0.0001$, 0 vs. 1 nM, 0 vs. 100 nM, 0 vs. 500 nM. (N,O) The summary bar graph of the HEK293 cells’ viability without hKv1.3 expression (N) and with hKv1.3 expression (O) under 1 h of ShK (0, 0.01, 1, 100, or 500 nM) treatment. (O–Q) The summary bar graph of the HEK293 cells’ viability without hKv1.3 expression (P) and with hKv1.3 expression (Q) under 1 h of NnK-1 (0, 0.01, 1, 100, or 500 nM) treatment. Data are the means \pm SEM.

We also found that NnK-1 (100 nM) significantly inhibited the current amplitude of hKv1.3, hKv1.4, and hKv1.5, but not that of hKv1.1, hKv3.1, and hKv11.1 (Figure 4, $* p < 0.05$, $** p < 0.01$, $*** p < 0.001$). These results implied that hKv1.3, hKv1.4, and hKv1.5 had a similar structure. The structure of hKv1.3, hKv1.4, and hKv1.5 has been recently studied [31]. These channels exhibit a similar overall structure, characterized by six transmembrane segments (S1–S6), with the S4 segment serving as the voltage sensor and the pore-forming region located between S5 and S6. Kv1.3 consists of four alpha subunits, each containing the six transmembrane segments. The S4 segment functions as the voltage sensor, housing positively charged amino acids that respond to changes in membrane potential. The pore region, formed by the S5 and S6 segments, facilitates the passage of potassium ions through the membrane. Similarly, Kv1.4 comprises four alpha subunits with six transmembrane segments. Kv1.5 channels also share the general structure of the Kv1 family channels, featuring six transmembrane segments per alpha subunit. It is intriguing that these three isoforms share structural similarities despite being expressed in different cell types or tissues. For instance, hKv1.3 channels are widely expressed in various tissues, including immune cells (such as T lymphocytes), neurons, and other cell types [12,32]; hKv1.4 channels are widely expressed in various tissues, including the nervous system, skeletal muscle, and heart [33,34]; while hKv1.5 channels are predominantly expressed in the heart [35,36].

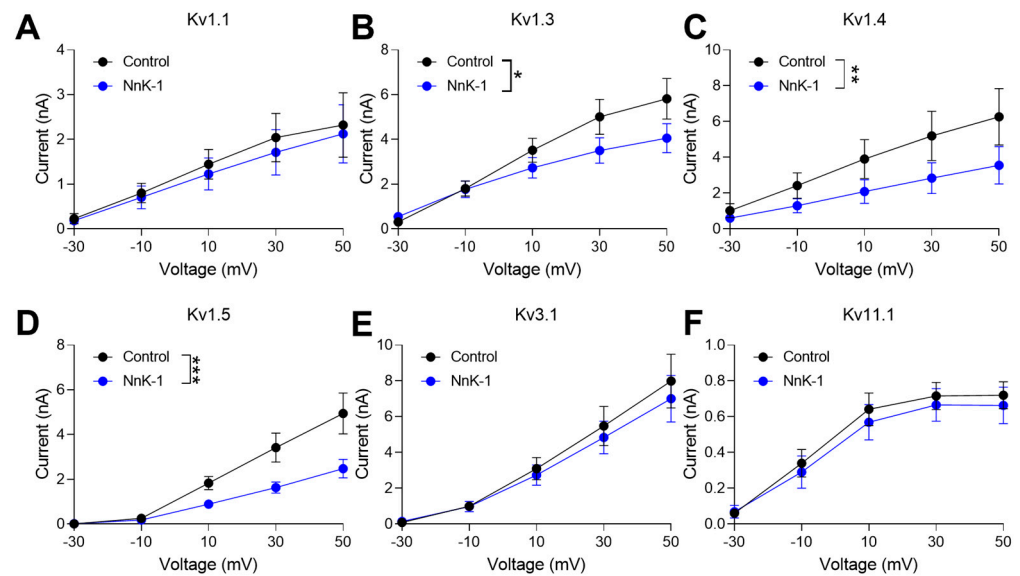


Figure 4. Inhibitory effect of NnK-1 on the activation of hKv channels. (A) Representative IV curves in the presence of 100 nM NnK-1 with respect to hKv1.1. Two-way ANOVA, interaction between the voltage and group $F(4, 20) = 0.03, p = 0.99$; voltage $F(4, 20) = 7.184, p < 0.001$; group $F(1, 20) = 0.43, p = 0.52$. (B) Representative IV curves in the presence of 100 nM NnK-1 with respect to hKv1.3. Two-way ANOVA, interaction between the voltage and group $F(4, 70) = 1.32, p = 0.27$; voltage $F(4, 70) = 22.81, p < 0.0001$; group $F(1, 70) = 5.03, * p < 0.05$. (C) Representative IV curves in the presence of 100 nM NnK-1 with respect to hKv1.4. Two-way ANOVA, interaction between the voltage and group $F(4, 30) = 0.49, p = 0.74$; voltage $F(4, 30) = 6.18, p < 0.001$; group $F(1, 30) = 8.17, ** p < 0.01$. (D) Representative IV curves in the presence of 100 nM NnK-1 with respect to hKv1.5. Two-way ANOVA, interaction between the voltage and group $F(4, 30) = 3.65, p < 0.05$; voltage $F(4, 30) = 30.85, p < 0.0001$; group $F(1, 30) = 17.51, *** p < 0.001$. (E) Representative IV curves in the presence of 100 nM NnK-1 with respect to hKv3.1. Two-way ANOVA, interaction between the voltage and group $F(4, 40) = 0.14, p = 0.97$; voltage $F(4, 40) = 26.93, p < 0.0001$; group $F(1, 40) = 0.56, p = 0.46$. (F) Representative IV curves in the presence of 100 nM NnK-1 with respect to hKv11.1. Two-way ANOVA, interaction between the voltage and group $F(4, 40) = 0.07, p = 0.99$; voltage $F(4, 40) = 23.68, p < 0.0001$; group $F(1, 40) = 0.75, p = 0.39$. Data are the means \pm SEM.

2.3. Structural Similarity between Sea Anemone ShKs and Jellyfish NnK-1

The amino acid sequences of the voltage-gated potassium channel blockers identified in sea anemones (ShK, BgK, HmK, AeK, AsKs, OsPTx2a, and AETxK1) and that in the jellyfish (NnK-1) were compared (Figure 5). The aspartic acid (D) in the third position of the peptide is conserved in the ShK analogs from both sea anemones and jellyfish. The one-amino-acid residues (T) located just before the fifth cysteine were also conserved in all the sequences. However, the positions of the two potential key binding residues (KY) were conserved in the sea anemone peptides but not in the jellyfish peptide. Therefore, three residues (^3Asp , ^{25}Lys , and ^{34}Thr in NnK-1) were likely to be essential for the binding of the toxin to the voltage-gated potassium channels. A peptide with these three amino acids, substituted with ^3Glu , ^{25}Arg , and ^{34}Met , named NnK-1 mu, was synthesized. Then, an electrophysiological assay was carried out with this peptide to confirm whether these three amino acid residues had a crucial role in the binding of the toxins to the voltage-gated potassium channels.

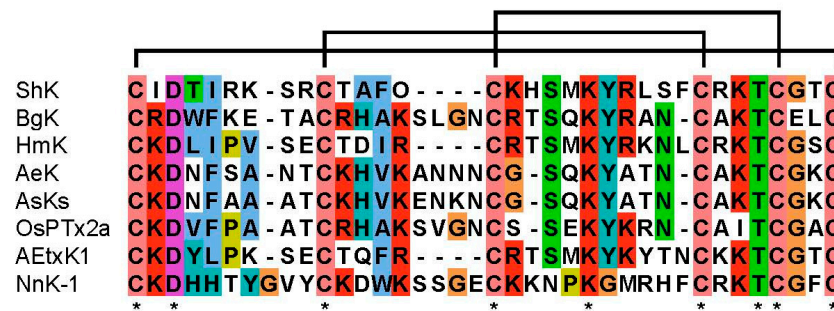


Figure 5. Multiple-sequence alignment of six sea anemone peptides and one jellyfish peptide, all of which show Kv1.3-blocking activity. ShK (from *Stichodactyla helianthus*), BgK (from *Bunodosoma granulifera*), HmK (from *Heteractis magnifica*), AeK (from *Actinia equina*), AsKs (from *Anemonia sulcata*), OsPtx2a (from *Oulactis* sp.), AEtXK1 (from *Anemonia erythraea*), and NnK-1 (from *N. nomurai*). Conserved amino acid residue marked with an asterisk.

Another peptide, NnK-1 w/o d, which had the same amino acid residues but without three pairs of disulfide bonds, was also synthesized to test whether the disulfide bonds were still intact in the synthetic NnK-1 after being dissolved in a solution. The results showed that neither NnK-1 mu nor NnK-1 w/o d inhibited the current amplitudes of hKv1.3 (Figure 6, * $p < 0.05$). Thus, the three residues and three pairs of disulfide bonds were necessary for potassium-channel-blocking activity, and the disulfide bonds in synthetic NnK-1 were maintained even when dissolved in a solution.

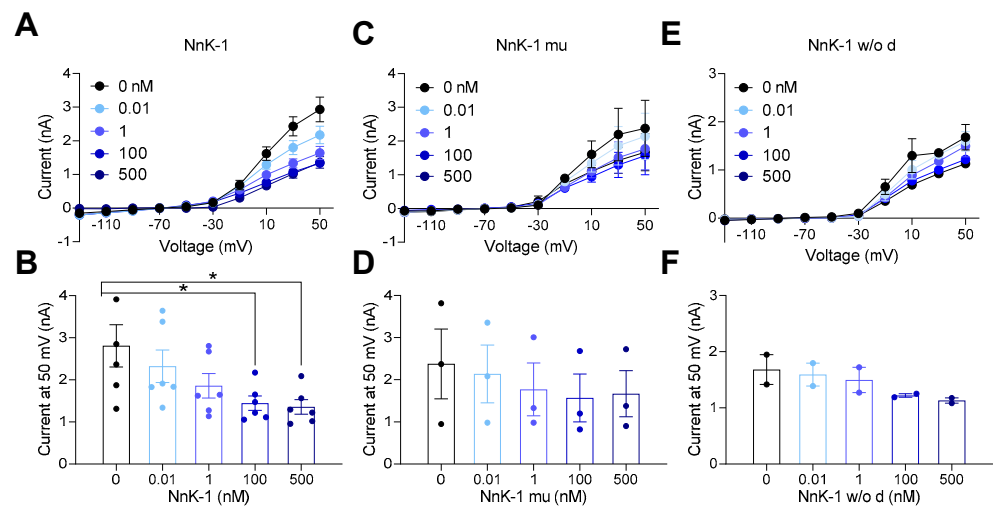


Figure 6. Inhibitory effects of NnK-1 analogs on the activation of hKv1.3 channels. (A) Representative IV curves in the presence of NnK-1 (0, 0.01, 1, 100, or 500 nM). (B) The summary bar graphs of current amplitudes at 50 mV in the presence of NnK-1 (0, 0.01, 1, 100, or 500 nM). One-way ANOVA, $F(4, 25) = 3.42$, $p < 0.05$, followed by Dunnett's post hoc test, * $p < 0.05$, 0 vs. 100 nM, 0 vs. 500 nM. (C) Representative IV curves in the presence of NnK-1 mu (0, 0.01, 1, 100, or 500 nM). (D) The summary bar graphs of current amplitudes at 50 mV in the presence of NnK-1 mu (0, 0.01, 1, 100, or 500 nM). One-way ANOVA, $F(4, 10) = 0.27$, $p = 0.89$. (E) Representative IV curves in the presence of NnK-1 w/o d (0, 0.01, 1, 100, or 500 nM). (F) The summary bar graphs of current amplitudes at 50 mV in the presence of NnK-1 w/o d (0, 0.01, 1, 100, or 500 nM). One-way ANOVA, $F(4, 5) = 1.71$, $p = 0.28$. Data are the means \pm SEM.

Meanwhile, the Shk-like peptides PcShK3 and AmAMP1 have been identified in corals. PcShK3 exerts both neuro- and cardioprotective effects in zebrafish [5], and AmAMP1 has antimicrobial activity [26]. Moreover, peptides with a cysteine-rich ShK motif that are expressed in neurons have been identified in *Nematostella vectensis*, a sea anemone model organism, together with a peptide expressed in nematocysts [37]. The position of aspartic

acid (D) is conserved in ShK peptides, and it has both toxic and other functions (Figure 7). However, the KT motif is only conserved in ShK peptides classified as toxins (Figure 7).

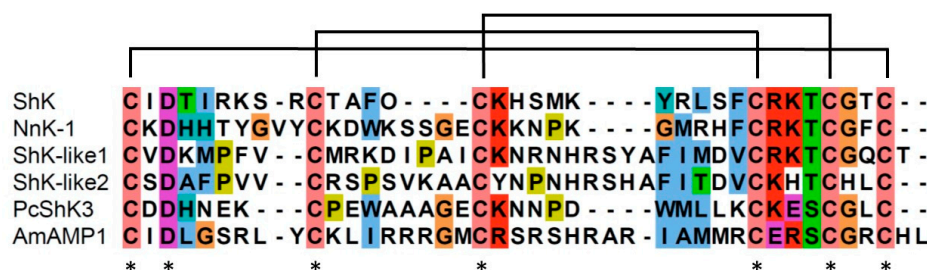


Figure 7. Multiple-sequence alignment of six ShK peptides. ShK, NnK-1, and ShK-like 1 peptides (from *Nematostella vectecsis*) are known to be toxins. ShK-like 2 (from *N. vectecsis*) is expressed in neurons, PcShK3 (from *Palythoa cariboeorum*) has neuro- and cardioprotective functions, and AmAMP1 (from *Acropora millepora*) has antimicrobial activity. Conserved amino acid residue marked with an asterisk.

In conclusion, we successfully identified and characterized a new voltage-gated potassium channel blocker in jellyfish, NnK-1, which interacts with three different voltage-gated potassium channels (hKv1.3, hKv 1.4, and hKv1.5). The discovery of a peptide that interacts with multiple voltage-gated potassium channels has significant implications for our knowledge of ion channel function, drug discovery, and potential therapeutic applications in various physiological and pathophysiological contexts. We also showed that using synthetic peptides based on genomic information, rather than purified peptides, is an efficient way to identify the biomaterials that can be developed for therapeutic application in the treatment of human diseases.

3. Materials and Methods

3.1. In Silico Identification of ShK-Like Peptide Genes in *N. nomurai*

The ShK domains (PF01549.26) of *N. nomurai* genes were identified with the Protein Families database (Pfam ver. 34.0). We confirmed the number of cysteine residues in the ShK domains and the presence of basic residues within the 10 amino acids flanking the ShK domains. Finally, we manually selected the ShK-like peptides to be synthesized.

3.2. Peptide Synthesis

NnK-1, NnK-1 mu, and NnK-1 w/o d (Table 1) were synthesized with a standard solid-phase methodology, followed by trifluoroacetic acid–anisole (81.5% TFA + 2.5% EDT + 5% H₂O + 5% phenol + 5% thioanisole + 1% TIS) cleavage and high-performance liquid chromatographic purification (Figure S1). Three disulfide bridges formed between Cys1 and Cys38, Cys11 and Cys31, and Cys20 and Cys35 but not in NnK-1 w/o d. The molecular weight of the synthetic peptide was confirmed with matrix-assisted laser desorption–ionization–time-of-flight (MALDI-TOF)–mass spectrometry (MS) (Shimadzu LCMS-2020, Kyoto, Japan) (Figures S2–S4). The peptide was synthesized by Pepmic Co. Ltd. (Suzhou, China).

Table 1. The primary structure of the synthetic peptides used in the assays.

Name	Sequence	Disulfide Bonds
NnK-1	CKDHHTYGVYCKDWKSSGECKKNPKGMRHFRCRKTCTGFC	O
NnK-1-mu	CKEHHTYGVYCKDWKSSGECKKNPRGMRHFRCRKMCGFC	O
NnK-1-w/o d	CKDHHTYGVYCKDWKSSGECKKNPKGMRHFRCRKTCTGFC	X

3.3. Cloning hKv cDNAs and Construction of hKv Expression Vectors

The primer sets used to amplify the hKvs (*hKv1.1*, *hKv1.3*, *hKv1.4*, *hKv1.5*, *hKv3.1*, and *hKv11.1*) gene are provided in Table 2. The amplification was performed in the Veriti™ 96-Well Fast Thermal Cycler (Applied Biosystems, Waltham, MA, USA) with a thermal cycling program consisting of predenaturation for 3 min at 95 °C, followed by 30 cycles of denaturation for 30 s at 95 °C, annealing for 30 s at 58 °C, and extension for 30 s at 72 °C, with a final extension for 3 min at 72 °C. A Human cDNA Clone Set (OriGene Technologies GmbH, Herford, Germany) was used as the template. A MCS (multi-cloning site) digested from the pAAV-MCS vector (Cell Biolabs, San Diego, CA, USA) was ligated into the pIRES2-EGFP vector (Clontech Laboratories, Mountain View, CA, USA) to form pAAV-CMV-IRES2-EGFP. The PCR products were ligated into the pAAV-CMV-IRES2-EGFP vector at the NheI and SalI sites to construct pAAV-CMV-hKv-IRES2-EGFP.

Table 2. The primer sets used to amplify the hKv channel genes with polymerase chain reaction.

Gene	Primer	Sequence
<i>hKv1.3</i>	NheI-Kv1.3-F SalI-Kv1.3-R	5'-TTTGCTAGCGCCACCATGGACGAGCGC-3' 5'-TTTGTCGACCTAAACATCGGTGAATATCTTTT-3'
<i>hKv1.1</i>	NheI-Kv1.1-F SalI-Kv1.1-R	5'-AACCGTCAGATCCGCTAGCGCCACCATGACGGTGATGTCTGGG-3' 5'-GAGGGGCGGTACCGTCGACTTAAACATCGGTGACGATAGC-3'
<i>hKv1.4</i>	NheI-Kv1.4-F SalI-Kv1.4-R	5'-TGAACCGTCAGATCCGCTAGCGCCACCATGGAGGTTGCAATGGTG-3' 5'-GAGAGGGGCGGTACCGTCGACTCACACATCAGTCTCCAC-3'
<i>hKv1.5</i>	NheI-Kv1.5-F SalI-Kv1.5-R	5'-AACCGTCAGATCCGCTAGCGCCACCATGGAGATCGCCCTGGTG-3' 5'-GAGGGGCGGTACCGTCGACTCACAAATCTGTTCCCG-3'
<i>hKv3.1</i>	NheI-Kv3.1-F SalI-Kv3.1-R	5'- AACCGTCAGATCCGCTAGCGCCACCATGGGCCAAGGGGACGAG-3' 5'-GAGGGGCGGTACCGTCGACTCAAGTCACTCTCACAGC-3'
<i>hKv11.1</i>	NheI-Kv11.1-F SalI-Kv11.1-R	5'-AGTGAACCGTCAGATCCGCTAGCGCCACCATGCCGGTGCGGAGGGGC-3' 5'-GGGAGAGGGGCGGTACCGTCGACCTAACTGCCGGGTCCGAG-3'

3.4. Preparation of hKv-Vector-Transformed HEK293 Cells

The HEK293 cells were transfected with pAAV-CMV-hKv-IRES2-EGFP (2 µg) using Effectene Transfection Reagent (Qiagen, Hilden, Germany) for 12–18 h. The transfectants (1×10^5 /mL) were seeded onto 12 mm coverslips coated with 0.01 mg/mL poly-D-lysine for 2–3 h.

3.5. Current Recording

The HEK293 cells expressing AAV-CMV-hKv-IRES2-EGFP were reseeded onto coverslips. The HEK293 transfectants were monitored for their green fluorescence and used as patch cells. Patch pipettes were filled with an internal solution (140 mM potassium gluconate, 10 mM HEPES, 0.2 mM ATP, and 0.06 mM GTP). An external solution [130 mM NaCl, 10 mM HEPES, 3 mM KCl, 1.5 mM D-glucose, 10 mM sucrose, 24 mM CaCl₂, 1.5 mM MgCl₂·6H₂O, osmolarity 320 mmol/kg (pH 7.2)] was used as the basic buffer. Psora4, ShK, or NnK-1 (0, 0.01, 1, 100, or 500 nM) was bath-applied for 2 min to block the currents recorded from the HEK293 cells expressing AAV-CMV-hKv-IRES2-EGFP with voltages ranging from −130 to 50 mV in the increments of 20 mV and 0.6 s. Whole-cell patch recordings from cultured cortical neurons under voltage-clamp conditions (holding potential of −70 mV) were made with the Multiclamp 700 B microelectrode amplifier (Automate Scientific Inc., Berkeley, CA, USA) digitized with a Digidata 1322 A data acquisition system (Molecular Devices Limited, San Jose, CA, USA). In this study, all electrophysiological data from the cultured cells were obtained at a temperature of 23–25 °C and maintained with the CL-100 Temperature Controller (Warner Instruments LLC, Hamden, CT, USA).

3.6. Cell Viability Assay

The cell viability of the HEK293 cells was assessed with a Cell Counting Kit-8 (CCK-8, DJDB4000X, Dojindo laboratory, Kumamoto, Japan). Both the HEK293 cells and HEK293 cells expressing AAV-CMV-hKv-IRES2-EGFP were seeded onto a 96-well plate (1×10^4 cells/well). After 24 h of incubation, ShK, NnK-1, NnK-1 mu, and NnK-1 w/o d (0, 0.01, 1, 100, or 500 nM) were used to treat the cells in each well for 1 h. After that, a dye solution was used to treat the cells for 2 h, and the absorbance was measured at 450 nm using a microplate reader (GloMax explorer multimode, Promega, Madison, WI, USA).

Supplementary Materials: The following supporting information can be downloaded at: <https://www.mdpi.com/article/10.3390/md22050217/s1>, Figure S1. Results from Pepmic Co. Ltd. for the purification of synthetic NnK-1 using high-performance liquid chromatography. Figure S2. Mass spectrometry analysis conducted by Pepmic Co. Ltd. illustrating the results subsequent to the formation of the first pair of disulfide bonds. Figure S3. Mass spectrometry analysis conducted by Pepmic Co. Ltd. illustrating the results subsequent to the formation of the second pair of disulfide bonds. Figure S4. Mass spectrometry analysis conducted by Pepmic Co. Ltd. illustrating the results subsequent to the formation of the third pair of disulfide bonds.

Author Contributions: Y.-J.K. and D.H.W., electrophysiological analysis; Y.J., N.L., and H.W., data analyses and manuscript preparation; S.E.L., vector construction; J.K. and J.-P.C., bioinformatic analyses; D.H.W. and S.Y., study design, manuscript preparation, and supervision. All authors have read and agreed to the published version of the manuscript.

Funding: This work was supported by the Marine Biotics Project (202110469) funded by the Ministry of Oceans and Fisheries, a grant (1711195891, KK-2313) from the Korea Institute of Toxicology (KIT) Research Program, and a grant 23212MFDS216 (1475014003, IP-2305) from the Ministry of Food and Drug Safety in 2023.

Institutional Review Board Statement: Not applicable.

Data Availability Statement: The data that support the findings of this study are available in the figures of the article.

Conflicts of Interest: The authors declare no conflicts of interest.

References

- Jouiaei, M.; Yanagihara, A.A.; Madio, B.; Nevalainen, T.J.; Alewood, P.F.; Fry, B.G. Ancient Venom Systems: A Review on Cnidaria Toxins. *Toxins* **2015**, *7*, 2251–2271. [[CrossRef](#)]
- Brinkman, D.L.; Jia, X.; Potriquet, J.; Kumar, D.; Dash, D.; Kvaskoff, D.; Mulvenna, J. Transcriptome and venom proteome of the box jellyfish *Chironex fleckeri*. *BMC Genom.* **2015**, *16*, 407. [[CrossRef](#)]
- Choudhary, I.; Hwang, D.H.; Lee, H.; Yoon, W.D.; Chae, J.; Han, C.H.; Yum, S.; Kang, C.; Kim, E. Proteomic Analysis of Novel Components of *Nemopilema nomurai* Jellyfish Venom: Deciphering the Mode of Action. *Toxins* **2019**, *11*, 153. [[CrossRef](#)]
- Wang, C.; Wang, B.; Wang, B.; Wang, Q.; Liu, G.; Wang, T.; He, Q.; Zhang, L. Unique Diversity of Sting-Related Toxins Based on Transcriptomic and Proteomic Analysis of the Jellyfish *Cyanea capillata* and *Nemopilema nomurai* (Cnidaria: Scyphozoa). *J. Proteome Res.* **2019**, *18*, 436–448. [[CrossRef](#)] [[PubMed](#)]
- Liao, Q.; Gong, G.; Siu, S.W.I.; Wong, C.T.T.; Yu, H.; Tse, Y.C.; Radis-Baptista, G.; Lee, S.M. A Novel ShK-Like Toxic Peptide from the Transcriptome of the Cnidarian *Palythoa caribaeorum* Displays Neuroprotection and Cardioprotection in Zebrafish. *Toxins* **2018**, *10*, 238. [[CrossRef](#)] [[PubMed](#)]
- Kim, H.M.; Weber, J.A.; Lee, N.; Park, S.G.; Cho, Y.S.; Bhak, Y.; Lee, N.; Jeon, Y.; Jeon, S.; Luria, V.; et al. The genome of the giant Nomura's jellyfish sheds light on the early evolution of active predation. *BMC Biol.* **2019**, *17*, 28. [[CrossRef](#)]
- Lee, H.; Bae, S.K.; Kim, M.; Pyo, M.J.; Kim, M.; Yang, S.; Won, C.K.; Yoon, W.D.; Han, C.H.; Kang, C.; et al. Anticancer Effect of *Nemopilema nomurai* Jellyfish Venom on HepG2 Cells and a Tumor Xenograft Animal Model. *Evid. Based Complement. Altern. Med.* **2017**, *2017*, 2752716. [[CrossRef](#)]
- Choudhary, I.; Lee, H.; Pyo, M.J.; Heo, Y.; Chae, J.; Yum, S.S.; Kang, C.; Kim, E. Proteomic Investigation to Identify Anticancer Targets of *Nemopilema nomurai* Jellyfish Venom in Human Hepatocarcinoma HepG2 Cells. *Toxins* **2018**, *10*, 194. [[CrossRef](#)]
- Jan, L.Y.; Jan, Y.N. Voltage-gated potassium channels and the diversity of electrical signalling. *J. Physiol.* **2012**, *590*, 2591–2599. [[CrossRef](#)]
- Finol-Urdaneta, R.K.; Belovanovic, A.; Micic-Vicovac, M.; Kinsella, G.K.; McArthur, J.R.; Al-Sabi, A. Marine Toxins Targeting Kv1 Channels: Pharmacological Tools and Therapeutic Scaffolds. *Mar. Drugs* **2020**, *18*, 173. [[CrossRef](#)]

11. Wulff, H.; Knaus, H.G.; Pennington, M.; Chandy, K.G. K⁺ channel expression during B cell differentiation: Implications for immunomodulation and autoimmunity. *J. Immunol.* **2004**, *173*, 776–786. [[CrossRef](#)]
12. Beeton, C.; Wulff, H.; Standifer, N.E.; Azam, P.; Mullen, K.M.; Pennington, M.W.; Kolski-Andreaco, A.; Wei, E.; Grino, A.; Counts, D.R.; et al. Kv1.3 channels are a therapeutic target for T cell-mediated autoimmune diseases. *Proc. Natl. Acad. Sci. USA* **2006**, *103*, 17414–17419. [[CrossRef](#)]
13. Chandy, K.G.; Sanches, K.; Norton, R.S. Structure of the voltage-gated potassium channel K(V)1.3: Insights into the inactivated conformation and binding to therapeutic leads. *Channels* **2023**, *17*, 2253104. [[CrossRef](#)]
14. Chhabra, S.; Chang, S.C.; Nguyen, H.M.; Huq, R.; Tanner, M.R.; Londono, L.M.; Estrada, R.; Dhawan, V.; Chauhan, S.; Upadhyay, S.K.; et al. Kv1.3 channel-blocking immunomodulatory peptides from parasitic worms: Implications for autoimmune diseases. *FASEB J.* **2014**, *28*, 3952–3964. [[CrossRef](#)]
15. Chandy, K.G.; Norton, R.S. Peptide blockers of K(v)1.3 channels in T cells as therapeutics for autoimmune disease. *Curr. Opin. Chem. Biol.* **2017**, *38*, 97–107. [[CrossRef](#)]
16. Perez-Verdaguer, M.; Capera, J.; Serrano-Novillo, C.; Estadella, I.; Sastre, D.; Felipe, A. The voltage-gated potassium channel Kv1.3 is a promising multitargeted therapeutic target against human pathologies. *Expert. Opin. Ther. Targets* **2016**, *20*, 577–591. [[CrossRef](#)]
17. Shen, B.; Cao, Z.; Li, W.; Sabatier, J.M.; Wu, Y. Treating autoimmune disorders with venom-derived peptides. *Expert. Opin. Biol. Ther.* **2017**, *17*, 1065–1075. [[CrossRef](#)]
18. Tarcha, E.J.; Olsen, C.M.; Probst, P.; Peckham, D.; Munoz-Elias, E.J.; Kruger, J.G.; Iadonato, S.P. Safety and pharmacodynamics of dalazatide, a Kv1.3 channel inhibitor, in the treatment of plaque psoriasis: A randomized phase 1b trial. *PLoS ONE* **2017**, *12*, e0180762. [[CrossRef](#)]
19. Castaneda, O.; Sotolongo, V.; Amor, A.M.; Stocklin, R.; Anderson, A.J.; Harvey, A.L.; Engstrom, A.; Wernstedt, C.; Karlsson, E. Characterization of a potassium channel toxin from the Caribbean Sea anemone *Stichodactyla helianthus*. *Toxicon* **1995**, *33*, 603–613. [[CrossRef](#)]
20. Tudor, J.E.; Pallaghy, P.K.; Pennington, M.W.; Norton, R.S. Solution structure of ShK toxin, a novel potassium channel inhibitor from a sea anemone. *Nat. Struct. Biol.* **1996**, *3*, 317–320. [[CrossRef](#)]
21. Gendeh, G.S.; Young, L.C.; de Medeiros, C.L.; Jeyaseelan, K.; Harvey, A.L.; Chung, M.C. A new potassium channel toxin from the sea anemone *Heteractis magnifica*: Isolation, cDNA cloning, and functional expression. *Biochemistry* **1997**, *36*, 11461–11471. [[CrossRef](#)]
22. Cotton, J.; Crest, M.; Bouet, F.; Alessandri, N.; Gola, M.; Forest, E.; Karlsson, E.; Castaneda, O.; Harvey, A.L.; Vita, C.; et al. A potassium-channel toxin from the sea anemone *Bunodosoma granulifera*, an inhibitor for Kv1 channels. Revision of the amino acid sequence, disulfide-bridge assignment, chemical synthesis, and biological activity. *Eur. J. Biochem.* **1997**, *244*, 192–202. [[CrossRef](#)]
23. Minagawa, S.; Ishida, M.; Nagashima, Y.; Shiomi, K. Primary structure of a potassium channel toxin from the sea anemone *Actinia equina*. *FEBS Lett.* **1998**, *427*, 149–151. [[CrossRef](#)]
24. Krishnarajuna, B.; Villegas-Moreno, J.; Mitchell, M.L.; Csoti, A.; Peigneur, S.; Amero, C.; Pennington, M.W.; Tytgat, J.; Panyi, G.; Norton, R.S. Synthesis, folding, structure and activity of a predicted peptide from the sea anemone *Oulactis* sp. with an ShKT fold. *Toxicon* **2018**, *150*, 50–59. [[CrossRef](#)]
25. Sunanda, P.; Krishnarajuna, B.; Peigneur, S.; Mitchell, M.L.; Estrada, R.; Villegas-Moreno, J.; Pennington, M.W.; Tytgat, J.; Norton, R.S. Identification, chemical synthesis, structure, and function of a new Kv1 channel blocking peptide from *Oulactis* sp. *Peptide Sci.* **2018**, *110*, e24073. [[CrossRef](#)]
26. Mason, B.; Cooke, I.; Moya, A.; Augustin, R.; Lin, M.F.; Satoh, N.; Bosch, T.C.G.; Bourne, D.G.; Hayward, D.C.; Andrade, N.; et al. AmAMP1 from *Acropora millepora* and damicornin define a family of coral-specific antimicrobial peptides related to the Shk toxins of sea anemones. *Dev. Comp. Immunol.* **2021**, *114*, 103866. [[CrossRef](#)]
27. Li, R.; Yu, H.; Xue, W.; Yue, Y.; Liu, S.; Xing, R.; Li, P. Jellyfish venomomics and venom gland transcriptomics analysis of *Stomolophus meleagris* to reveal the toxins associated with sting. *J. Proteomics* **2014**, *106*, 17–29. [[CrossRef](#)]
28. Ponce, D.; Brinkman, D.L.; Potriquet, J.; Mulvenna, J. Tentacle Transcriptome and Venom Proteome of the Pacific Sea Nettle, *Chrysaora fuscescens* (Cnidaria: Scyphozoa). *Toxins* **2016**, *8*, 102. [[CrossRef](#)]
29. Schwartz, T.W. Cellular peptide processing after a single arginyl residue. Studies on the common precursor for pancreatic polypeptide and pancreatic icosapeptide. *J. Biol. Chem.* **1987**, *262*, 5093–5099. [[CrossRef](#)]
30. Mitchell, M.L.; Tonkin-Hill, G.Q.; Morales, R.A.V.; Purcell, A.W.; Papenfuss, A.T.; Norton, R.S. Tentacle Transcriptomes of the Speckled Anemone (Actiniaria: Actiniidae: *Oulactis* sp.): Venom-Related Components and Their Domain Structure. *Mar. Biotechnol.* **2020**, *22*, 207–219. [[CrossRef](#)]
31. Rohaim, A.; Vermeulen, B.J.A.; Li, J.; Kummerer, F.; Napoli, F.; Blachowicz, L.; Medeiros-Silva, J.; Roux, B.; Weingarh, M. A distinct mechanism of C-type inactivation in the Kv-like KcsA mutant E71V. *Nat. Commun.* **2022**, *13*, 1574. [[CrossRef](#)]
32. Cahalan, M.D.; Chandy, K.G. The functional network of ion channels in T lymphocytes. *Immunol. Rev.* **2009**, *231*, 59–87. [[CrossRef](#)]
33. Rasband, M.N.; Park, E.W.; Vanderah, T.W.; Lai, J.; Porreca, F.; Trimmer, J.S. Distinct potassium channels on pain-sensing neurons. *Proc. Natl. Acad. Sci. USA* **2001**, *98*, 13373–13378. [[CrossRef](#)]
34. O'Donovan, B.; Adeluyi, A.; Anderson, E.L.; Cole, R.D.; Turner, J.R.; Ortinski, P.I. Altered gating of K(v)1.4 in the nucleus accumbens suppresses motivation for reward. *Elife* **2019**, *8*, e47870. [[CrossRef](#)]
35. Ding, W.G.; Xie, Y.; Toyoda, F.; Matsuura, H. Improved functional expression of human cardiac kv1.5 channels and trafficking-defective mutants by low temperature treatment. *PLoS ONE* **2014**, *9*, e92923. [[CrossRef](#)]

36. Nattel, S.; Maguy, A.; Le Bouter, S.; Yeh, Y.H. Arrhythmogenic ion-channel remodeling in the heart: Heart failure, myocardial infarction, and atrial fibrillation. *Physiol. Rev.* **2007**, *87*, 425–456. [[CrossRef](#)]
37. Sachkova, M.Y.; Landau, M.; Surm, J.M.; Macrander, J.; Singer, S.A.; Reitzel, A.M.; Moran, Y. Toxin-like neuropeptides in the sea anemone *Nematostella* unravel recruitment from the nervous system to venom. *Proc. Natl. Acad. Sci. USA* **2020**, *117*, 27481–27492. [[CrossRef](#)]

Disclaimer/Publisher’s Note: The statements, opinions and data contained in all publications are solely those of the individual author(s) and contributor(s) and not of MDPI and/or the editor(s). MDPI and/or the editor(s) disclaim responsibility for any injury to people or property resulting from any ideas, methods, instructions or products referred to in the content.